

# Entanglement harvesting of circularly accelerated detectors with a reflecting boundary

Runhu Li<sup>1</sup>, Zixu Zhao<sup>\*1</sup>

<sup>1</sup>*School of Science, Xi'an University of Posts and Telecommunications, Xi'an 710121, China*

## Abstract

We study the properties of the transition probability for a circularly accelerated detector which interacts with the massless scalar fields in the presence of a reflecting boundary. As trajectory radius increases, the transition probability may exist some peaks in special circumstances, which lead to the possibility of same result for different trajectory radius with the same acceleration and energy gap. These behaviors can be characterized by some critical values. Furthermore, we analyze the entanglement harvesting phenomenon for two circularly accelerated detectors with a boundary. We consider that the two detectors are rotating around a common axis with the same acceleration, trajectory radius and angular velocity. When the detectors are close to the boundary, there may exist two peaks for entanglement harvesting. Interestingly, as trajectory radius increases, entanglement harvesting in some situations first decreases to zero, then maintains zero, and finally increases to a stable value. For a small energy gap, as the distance between the two detectors increases, the entanglement harvesting first takes zero at a larger distance between detectors and the boundary.

---

\* Corresponding author. zhaoyixu@yeah.net

## I. INTRODUCTION

In 1932, von Neumann completed mathematical foundations of non relativistic quantum description [1]. In 1935, Einstein, Podolsky and Rosen (EPR) attempted to show that “the wave function does not provide a complete description of the physical reality” [2]. The EPR paper inspired much discussion about the foundations of quantum mechanics. Following the EPR paper, Schrödinger used the word “Verschränkung” [3], and discussed the notion of “entanglement” [4]. Wu and Shaknov studied the angular correlation of scattered annihilation radiation [5]. A variant of the EPR thought experiment has been proposed [6–8]. In 1964, the Bell inequality showed that quantum physics predicts correlations that violate this inequality [9]. Freedman and Clauser performed the first rudimentary experiment designed to test Bell’s theorem in 1972, which was only a limited test [10]. For example, the experiment used polarizers that were preset. Aspect and his collaborators performed the Bell test which remove the limitation [11, 12]. Zeilinger team first obtain realization of quantum teleportation of an independent qubit [13].

In recent years, it has been realized that vacuum can be a resource of entanglement. Summers and Werner found that the vacuum state in free quantum field theory violates Bell’s inequalities maximally [14–16]. Valentini showed that a pair of initially uncorrelated atoms, separated by a distance  $R$ , develop non-local statistical correlations in a time  $t < R/c$ , which can be understood in terms of non-locally-correlated vacuum field fluctuations [17]. Reznik showed that entanglement persists between disconnected regions in the vacuum, and vacuum entanglement becomes a physical operational quantity, by transforming vacuum entanglement to pairs of probes or atom-like system [18]. Reznik, Retzker and Silman presented a physical effect of vacuum fluctuations which is associated with quantum nonlocality [19]. Entanglement can be used to detect spacetime curvature and quantum fields in the Minkowski vacuum are entangled with respect to local field modes [20]. Entanglement between the future and the past in the quantum vacuum has been studied [21]. Martín-Martínez and Menicucci considered the extraction of entanglement from a quantum field by coupling to local detectors and how this procedure can be used to distinguish curvature from heating by their entanglement signature [22]. Hu, Lin, and Louko studied relativistic quantum information in detectors-field interactions [23]. Martín-Martínez, Brown, Donnelly, and Kempf proposed a protocol by which entanglement can be extracted repeatedly from

a quantum field, and they called this protocol entanglement farming in analogy with prior work on entanglement harvesting [24]. Salton, Mann, and Menicucci studied entanglement harvested from a quantum field through local interaction with Unruh-DeWitt (UDW) detectors undergoing linear acceleration [25]. Pozas-Kerstjens and Martín-Martínez analyzed the harvesting of entanglement and classical correlations from the quantum vacuum to particle detectors [26].

The entanglement harvesting have been studied extensively [27–35]. Zhang and Yu studied entanglement harvesting for detectors in circular motion [33]. In this paper we will study the entanglement harvesting phenomenon of two circularly accelerated detectors with a reflecting boundary. The particle detector interacting with vacuum quantum fields can be depicted by using the well-known Unruh-DeWitt model [36]. We would like to further explore the role of parameters in detail.

The plan of the work is the following. In Sec. II, we review basic formulae for the UDW detectors locally interacting with vacuum scalar fields. In Sec. III, we will consider the transition probabilities of circularly accelerated UDW detectors with a reflecting boundary. In Sec. IV, we will study the entanglement harvesting phenomenon for a pair of coaxial accelerating detectors along circular trajectories with a reflecting boundary. We conclude in the last section with our main results. We employ the natural units  $\hbar = c = 1$  for convenience.

## II. THE BASIC FORMULAS

In this section, we will consider a pair of point-like two-level atoms (labeled by  $A$  and  $B$ ) interacting locally with a quantum scalar field. The two-level atom with the ground state  $|0\rangle_D$  and excited state  $|1\rangle_D$  separated by an energy gap  $\Omega_D$  can be modeled with the UDW detector, where the subscript  $D$  specifies which UDW detector we are considering. The spacetime trajectory  $x_D(\tau_D)$  of the detector is parametrized in terms of its proper time. Then the interacting Hamiltonian for such a detector locally coupling with a massless scalar field  $\phi[x_D(\tau_D)]$  has the following form in the interaction picture

$$H_D(\tau_D) = \lambda \chi_D(\tau_D) \left( e^{-i\Omega_D \tau_D} \sigma^- + e^{i\Omega_D \tau_D} \sigma^+ \right) \otimes \phi[x_D(\tau_D)] , \quad D \in \{A, B\} \quad (1)$$

where  $\lambda$  is the coupling strength and  $\chi_D(\tau_D) := e^{-\tau_D^2/(2\sigma_D^2)}$  is a Gaussian switching function which controls the duration of interaction via parameter  $\sigma_D$ . Particularly,  $\sigma^- = |0\rangle_D \langle 1|_D$  and  $\sigma^+ = |1\rangle_D \langle 0|_D$  denote the ladder operators acting on the Hilbert space of the detector.

We assume that detectors  $A$  and  $B$  in their ground states and the scalar field in vacuum state  $|0\rangle$  before the interaction begins. Therefore the initial joint state of the detectors and the field can be written as  $|\Psi\rangle = |0\rangle_A |0\rangle_B |0\rangle$ . We assume that the two detectors have completely identical energy gap  $\Omega = \Omega_A = \Omega_B$  and switching parameter  $\sigma = \sigma_A = \sigma_B$  for simplicity. According to the detector-field interaction Hamiltonian Eq. (1), the composite system (two detectors plus the field) will undergo the unitary evolution, where the evolution operator satisfies

$$U := \mathcal{T} \exp \left[ -i \int dt \left( \frac{d\tau_A}{dt} H_A(\tau_A) + \frac{d\tau_B}{dt} H_B(\tau_B) \right) \right], \quad (2)$$

here  $\mathcal{T}$  represents the time ordering operator. Based on the perturbation theory, in the basis  $\{|0\rangle_A |0\rangle_B, |0\rangle_A |1\rangle_B, |1\rangle_A |0\rangle_B, |1\rangle_A |1\rangle_B\}$ , the final reduced density matrix of the system (two detectors) can be obtained by tracing out the field degrees of freedom, after some manipulations [27, 29, 30]

$$\begin{aligned} \rho_{AB} &:= \text{tr}_\phi (U |\Psi\rangle \langle \Psi| U^\dagger) \\ &= \begin{pmatrix} 1 - P_A - P_B & 0 & 0 & X \\ 0 & P_B & C & 0 \\ 0 & C^* & P_A & 0 \\ X^* & 0 & 0 & 0 \end{pmatrix} + \mathcal{O}(\lambda^4). \end{aligned} \quad (3)$$

In the reduced density matrix  $\rho_{AB}$ , the transition probability  $P_D$  reads

$$P_D := \lambda^2 \iint d\tau_D d\tau'_D \chi_D(\tau_D) \chi_D(\tau'_D) e^{-i\Omega(\tau_D - \tau'_D)} W(x_D(\tau_D), x_D(\tau'_D)) \quad D \in \{A, B\}, \quad (4)$$

and quantities  $C$  and  $X$  which characterize nonlocal correlations read

$$C := \lambda^2 \iint dt dt' \frac{\partial \tau_B}{\partial t} \frac{\partial \tau_A}{\partial t'} \chi_B(\tau_B(t)) \chi_A(\tau_A(t')) e^{i[\Omega \tau_B(t) - \Omega \tau_A(t')]} W(x_A(t'), x_B(t)), \quad (5)$$

$$\begin{aligned} X &:= -\lambda^2 \iint_{t > t'} dt dt' \left[ \frac{\partial \tau_B}{\partial t} \frac{\partial \tau_A}{\partial t'} \chi_B(\tau_B(t)) \chi_A(\tau_A(t')) e^{-i[\Omega \tau_B(t) + \Omega \tau_A(t')]} W(x_A(t'), x_B(t)) \right. \\ &\quad \left. + \frac{\partial \tau_A}{\partial t} \frac{\partial \tau_B}{\partial t'} \chi_A(\tau_A(t)) \chi_B(\tau_B(t')) e^{-i[\Omega \tau_A(t) + \Omega \tau_B(t')]} W(x_B(t'), x_A(t)) \right], \end{aligned} \quad (6)$$

where  $W(x, x') := \langle 0 | \phi(x) \phi(x') | 0 \rangle$  denotes the Wightman function of the field.

Based on the entanglement harvesting protocol [25], we employ the concurrence as a measure of entanglement [37], which can quantify the entanglement harvested by the detectors via local interaction with the fields. For the  $X$ -like density matrix given in Eq. (3), the concurrence takes a form [27]

$$\mathcal{C}(\rho_{AB}) = 2 \max \{0, |X| - \sqrt{P_A P_B}\} + \mathcal{O}(\lambda^4). \quad (7)$$

The concurrence  $\mathcal{C}(\rho_{AB})$  depend on the non-local correlations  $X$  and the transition probabilities  $P_A$  and  $P_B$ , which is determined by the Wightman function of scalar fields. We will investigate the entanglement harvesting phenomenon for a pair of accelerated detectors moving in a circle near a boundary.

### III. THE TRANSITION PROBABILITIES OF CIRCULARLY ACCELERATED UDW DETECTORS NEAR THE REFLECTING BOUNDARY

In this section, we analyze the transition probability. For the convenience of discussion, we suppose that a plane boundary is located at  $z = 0$ , and the accelerated UDW detector performs circular motion parallel to the  $xy$ -plane with a distance  $\Delta z$  away from the boundary. The spacetime trajectory describing such detector parameterized by the proper time  $\tau_D$  is

$$x_D := \{t = \gamma_D \tau_D, \quad x = R_D \cos(\omega_D \gamma_D \tau_D), \quad y = R_D \sin(\omega_D \gamma_D \tau_D), \quad z = \Delta z\}, \quad (8)$$

where  $R_D$  is the radius of the circular trajectory and  $\omega_D$  represents the angular velocity of the detector moving in a circle, and  $\gamma_D = 1/\sqrt{1 - R_D^2 \omega_D^2}$  denotes the Lorentz factor. In the detector's frame, the magnitude of acceleration is  $a_D = \gamma_D^2 \omega_D^2 R_D = \gamma_D^2 v_D^2 / R_D$ , with the magnitude of linear velocity satisfies  $v_D = |\omega_D| R_D < 1$ . It should be noted that  $R_D$ ,  $\omega_D$ ,  $a_D$  and  $v_D$  are not completely independent.

In a four dimensional Minkowski spacetime, the Wightman function for massless scalar fields with a reflecting boundary can be given by [38]

$$W(x, x') = -\frac{1}{4\pi^2} \left[ \frac{1}{(t - t' - i\epsilon)^2 - (x - x')^2 - (y - y')^2 - (z - z')^2} - \frac{1}{(t - t' - i\epsilon)^2 - (x - x')^2 - (y - y')^2 - (z + z')^2} \right]. \quad (9)$$

Substitute the trajectory (8) into Eq. (9), we can get

$$W(\tau_D, \tau'_D) = -\frac{1}{4\pi^2} \left[ \frac{1}{(\gamma_D \Delta\tau - i\epsilon)^2 - 4R_D^2 \sin^2(\gamma_D \omega_D \Delta\tau/2)} - \frac{1}{(\gamma_D \Delta\tau - i\epsilon)^2 - 4R_D^2 \sin^2(\gamma_D \omega_D \Delta\tau/2) - 4\Delta z^2} \right], \quad (10)$$

where  $\Delta\tau = \tau_D - \tau'_D$ .

Substituting the Eq. (10) into Eq. (4), we get the expression for transition probability  $P_D$  (see Appendix A for detail)

$$P_D = K_D \int_0^\infty dx \frac{e^{-\alpha x^2} \cos(\beta x) (x^2 - \sin^2 x)}{x^2 (x^2 - v_D^2 \sin^2 x)} + \frac{\lambda^2 |\omega_D| \sigma}{4\pi^{3/2} \gamma} \text{PV} \int_0^\infty dx \frac{e^{-\alpha x^2} \cos(\beta x)}{x^2 - v_D^2 \sin^2(x) - \omega_D^2 \Delta z^2} + \frac{\lambda^2}{4\pi} \left[ e^{-\Omega^2 \sigma^2} - \sqrt{\pi} \Omega \sigma \text{Erfc}(\Omega \sigma) \right] + \frac{\lambda^2 |\omega_D| \sigma}{4\sqrt{\pi} \gamma} \frac{e^{-\alpha S^2} \sin(\beta S)}{2S - v_D^2 \sin(2S)}, \quad (11)$$

where

$$\alpha = \frac{1}{\sigma^2 \omega_D^2 \gamma_D^2} = \frac{R_D}{a_D \sigma^2}, \quad \beta = \frac{2\Omega}{\gamma_D |\omega_D|}, \quad K_D = \frac{\lambda^2 v_D^2 \gamma_D |\omega_D| \sigma}{4\pi^{3/2}} = \frac{\lambda^2 v_D a_D \sigma}{4\pi^{3/2} \gamma_D}, \quad (12)$$

and  $\text{Erfc}(x) = 1 - \text{Erf}(x)$  is the complementary the error function with  $\text{Erf}(x) := \int_0^x 2e^{-t^2} dt / \sqrt{\pi}$ .  $S$  is the solution of the equation  $x^2 - v_D^2 \sin^2 x - \omega_D^2 \Delta z^2 = 0$ .

To make a cross-comparison, we consider the following uniformly accelerated detector trajectory [25, 38–40]

$$x_D := \{t = a_D^{-1} \sinh(a_D \tau), \quad x = a_D^{-1} \cosh(a_D \tau), \quad y = 0, \quad z = \Delta z\}, \quad (13)$$

where  $a_D$  still denotes the magnitude of the linear constant acceleration.

We use the corresponding dimensionless in the unit of  $\sigma$ . In Fig. 1, we describe the transition probability as a function of  $R_D/\sigma$  for different  $a_D \sigma$  with fixed  $\Omega \sigma = \{0.10, 1.80\}$  and  $\Delta z/\sigma = \{0.20, 3.00, 10.00\}$ . For small  $\Omega \sigma = 0.10$  and small  $\Delta z/\sigma = 0.2$  in Fig. 1(a), as  $R_D/\sigma$  increases, the transition probability increases and goes to a stable nonzero value for a large  $a_D \sigma > a_{D_c} \sigma$  ( $a_{D_c} \sigma \approx 6.931$ ). As we decrease  $a_D \sigma$ , the transition probability first increases, then decreases, and finally increases to a stable value. With decreasing  $a_D \sigma$ , the transition probability first increases, then decreases to a stable value. There exists a single peak for not large  $a_D \sigma$ . However, it will increase to a stable value with a larger  $\Delta z/\sigma$  for any nonzero  $a_D \sigma$  as shown in Figs. 1(b) and 1(c). For a larger  $\Omega \sigma = 1.80$ , the transition

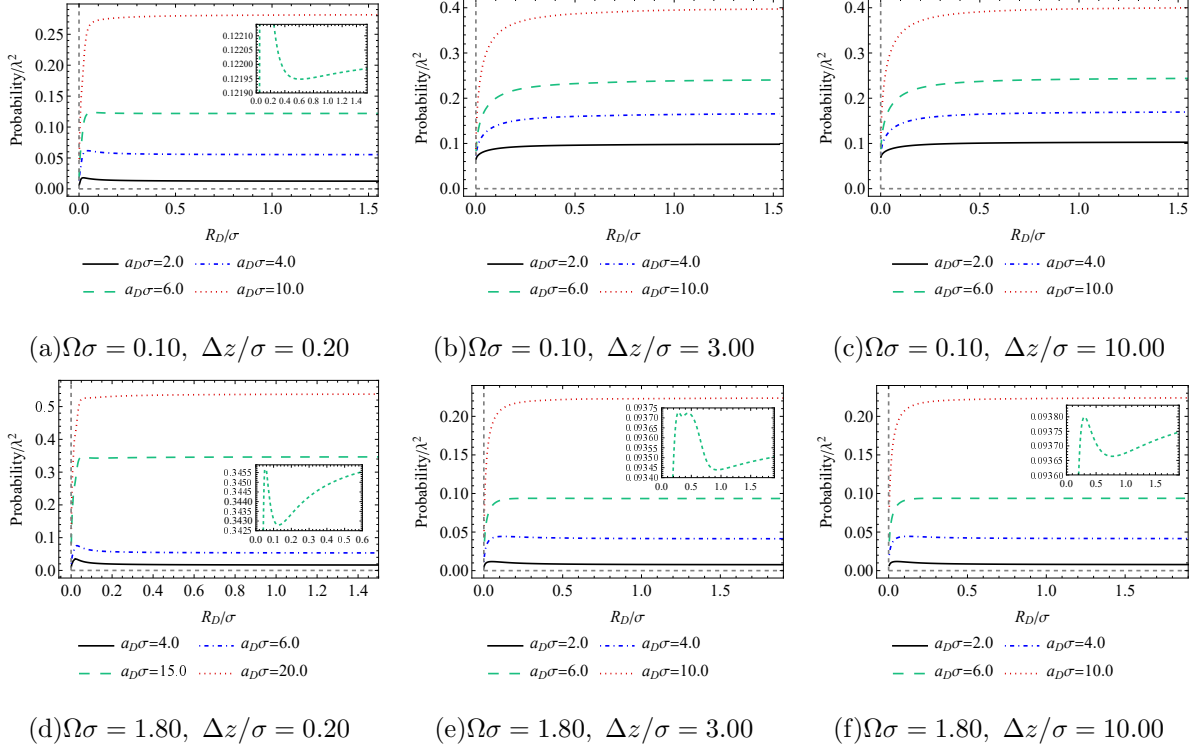


FIG. 1: The transition probability of UDW detector is plotted as a function of  $R_D/\sigma$  for different  $a_D\sigma$  with  $\Omega\sigma = \{0.10, 1.80\}$  and  $\Delta z/\sigma = \{0.20, 3.00, 10.00\}$ .

probability is similar to the case of Fig. 1(a) with small  $\Delta z/\sigma$ . As  $\Delta z/\sigma$  increases, there will exist more than one peak for some  $a_D\sigma$  as shown in Fig. 1(e). For a large  $\Delta z/\sigma$ , the feature is also similar to the case of Fig. 1(a).

We plot the transition probability of detector as a function of  $a_D\sigma$  with different  $\Delta z/\sigma$  and  $\Omega\sigma$  for the circular and linear motion in Fig. 2. The transition probability of detector is increasing function of acceleration. For a small  $\Omega\sigma$  such as  $\Omega\sigma = 0.10$  in the top row, there exists a critical value  $\Delta z_c/\sigma$  ( $\Delta z_c/\sigma \approx 0.814$ ). When  $\Delta z/\sigma < \Delta z_c/\sigma$ , as  $a_D\sigma$  increases, a larger transition probability can be obtained first for a smaller trajectory radius, which is opposite to the case of large  $a_D\sigma$ . As we amplify  $\Delta z/\sigma$ , the intersections are shifted to the left. When  $\Delta z/\sigma > \Delta z_c/\sigma$ , there is not intersection for all curves with nonzero  $a_D\sigma$ , which means a larger transition probability can be acquired for a larger trajectory radius with every nonzero  $a_D\sigma$ . However, with a larger  $\Omega\sigma > \Omega_c\sigma$  ( $\Omega_c\sigma \approx 0.707$ ) such as  $\Omega\sigma = 1.80$  in the bottom row, the curves always exist intersections with different  $R_D/\sigma$  for any  $\Delta z/\sigma$ . The transition probability for a large  $R_D/\sigma$  is close to the uniformly accelerated situation.

For a very large  $\Omega\sigma$ , the transition probability goes to zero, which can be seen from

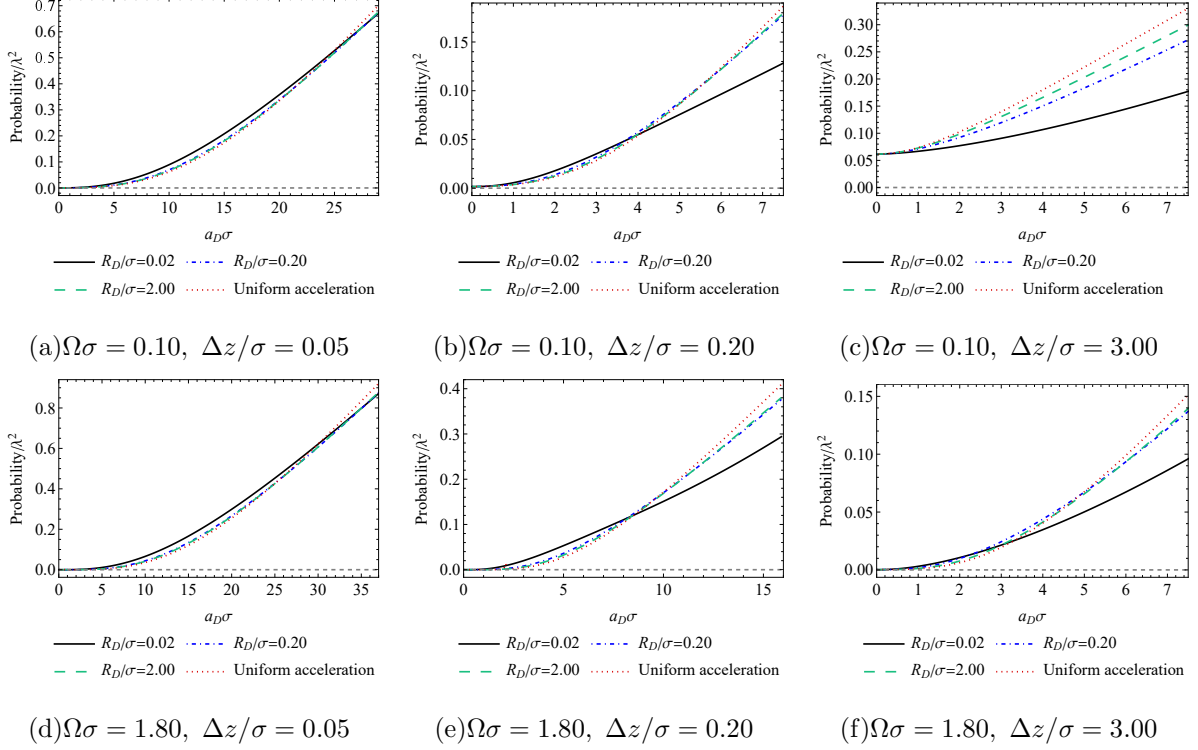


FIG. 2: The transition probability of UDW detector as a function of acceleration with  $\Omega\sigma = \{0.10, 1.80\}$  for  $R_D/\sigma = \{0.02, 0.20, 2.00\}$  and  $\Delta z/\sigma = \{0.05, 0.20, 3.00\}$ .

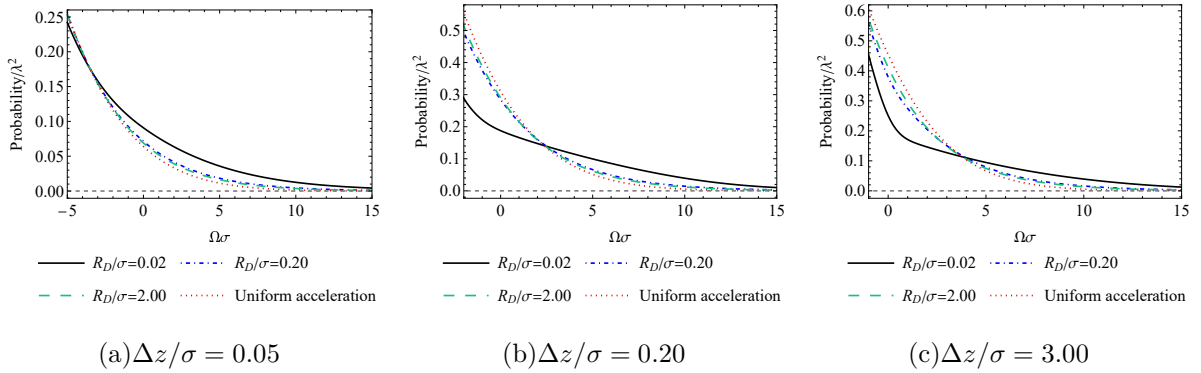


FIG. 3: The transition probability of UDW detector is plotted as a function of  $\Omega\sigma$  with  $a_D\sigma = 10.0$  and  $\Delta z/\sigma = \{0.05, 0.20, 3.00\}$  for both circularly and uniformly accelerated motion. The positive (negative) energy gaps correspond to that detector prepared in its ground (excited) state prior to interacting with the field.

Fig. 3. We depict the transition probability of detector as a function of  $\Omega\sigma$  in Fig. 3. The transition probability decreases with the increase of  $\Omega\sigma$ . As  $\Delta z/\sigma$  increases, the intersections are shifted to the right until not move.



#### IV. ENTANGLEMENT HARVESTING OF UDW DETECTORS IN THE CIRCULAR MOTION NEAR THE REFLECTING BOUNDARY

Now, we study the entanglement harvesting of two circularly accelerated detectors with a boundary. For simplicity, we mainly focus on the spacetime trajectories of the detectors in coaxial rotation (see Fig. 4).

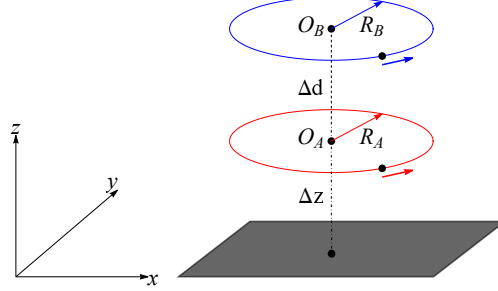


FIG. 4: The circular trajectories for two UDW detectors  $A$  and  $B$  in flat spacetime. Here, the boundary is in the  $xy$ -plane, and there is a common rotational axis of such two detectors.

We assume that detectors  $A$  and  $B$  with angular velocities  $\omega_A$  and  $\omega_B$  rotate around the common axis with the radii  $R_A$  and  $R_B$ . The spacetime trajectories of such two detectors can be parameterized by their proper time  $\tau_A$  and  $\tau_B$

$$\begin{aligned} x_A &:= \{t = \tau_A \gamma_A, \quad x = R_A \cos(\omega_A \tau_A \gamma_A), \quad y = R_A \sin(\omega_A \tau_A \gamma_A), \quad z = \Delta z\}, \\ x_B &:= \{t = \tau_B \gamma_B, \quad x = R_B \cos(\omega_B \tau_B \gamma_B), \quad y = R_B \sin(\omega_B \tau_B \gamma_B), \quad z = \Delta z + \Delta d\}, \end{aligned} \quad (14)$$

where  $\gamma_A$  and  $\gamma_B$  are corresponding Lorentz factors of detectors  $A$  and  $B$ , and  $\Delta d$  is the distance between two detectors.

We can get the transition probabilities of two detectors by using Eq. (11) and the spacetime trajectories (14). Substituting the trajectories Eq. (14) and the Wightman function Eq. (9) into Eq. (6), we get the nonlocal correlation term  $X$ . After some algebraic manipulations,  $X$  can be written as

$$\begin{aligned} X &= -\frac{\lambda^2 \sigma^2}{4\pi^2 \gamma_A \gamma_B} \int_{-\infty}^{\infty} d\tilde{u} \int_0^{\infty} d\tilde{s} \left\{ \exp \left[ \frac{-\gamma_A^2 \tilde{u}^2 - \gamma_B^2 (\tilde{s} - \tilde{u})^2}{2\gamma_A^2 \gamma_B^2} \right] \exp \left[ \frac{i(\tilde{s} - \tilde{u})\sigma\Omega}{\gamma_A} - \frac{i\tilde{u}\sigma\Omega}{\gamma_B} \right] \right. \\ &\quad \times \left( \frac{1}{f_{AB}(\tilde{u}, \tilde{s})} - \frac{1}{f_{AB}(\tilde{u}, \tilde{s}) + 4\Delta d \Delta z + 4\Delta z^2} \right) + \exp \left[ \frac{-\gamma_B^2 \tilde{u}^2 - \gamma_A^2 (\tilde{s} - \tilde{u})^2}{2\gamma_A^2 \gamma_B^2} \right] \\ &\quad \left. \times \exp \left[ \frac{i(\tilde{s} - \tilde{u})\sigma\Omega}{\gamma_B} - \frac{i\tilde{u}\sigma\Omega}{\gamma_A} \right] \left( \frac{1}{f_{BA}(\tilde{u}, \tilde{s})} - \frac{1}{f_{BA}(\tilde{u}, \tilde{s}) + 4\Delta d \Delta z + 4\Delta z^2} \right) \right\}, \end{aligned} \quad (15)$$

where the auxiliary functions are

$$f_{AB}(\tilde{u}, \tilde{s}) = \Delta d^2 + R_A^2 + R_B^2 - 2R_A R_B \cos(\tilde{u}\omega_A\sigma - \tilde{u}\omega_B\sigma - \tilde{s}\omega_A\sigma) - \sigma^2(\tilde{s} + i\epsilon)^2, \quad (16)$$

$$f_{BA}(\tilde{u}, \tilde{s}) = \Delta d^2 + R_A^2 + R_B^2 - 2R_A R_B \cos(\tilde{u}\omega_A\sigma - \tilde{u}\omega_B\sigma + \tilde{s}\omega_B\sigma) - \sigma^2(\tilde{s} + i\epsilon)^2. \quad (17)$$

We suppose that the two detectors are completely synchronously rotating around  $z$ -axis, i.e.,  $\omega_A = \omega_B = \omega$ , then Eq. (15) can be written as

$$X = -\frac{\lambda^2\sigma^2}{\pi^{3/2}\sqrt{2(\gamma_A^2 + \gamma_B^2)}} \exp\left[\frac{-\sigma^2\Omega^2(\gamma_A + \gamma_B)^2}{2(\gamma_A^2 + \gamma_B^2)}\right] \int_0^\infty d\tilde{s} \cos\left[\frac{\tilde{s}\sigma\Omega(\gamma_A - \gamma_B)}{\gamma_A^2 + \gamma_B^2}\right] \times \exp\left[\frac{-\tilde{s}^2}{2(\gamma_A^2 + \gamma_B^2)}\right] \left(\frac{1}{f(\tilde{u}, \tilde{s})} - \frac{1}{f(\tilde{u}, \tilde{s}) + 4\Delta d\Delta z + 4\Delta z^2}\right), \quad (18)$$

where

$$f(\tilde{u}, \tilde{s}) = \Delta d^2 + R_A^2 + R_B^2 - 2R_A R_B \cos(\tilde{s}\omega\sigma) - \sigma^2(\tilde{s} + i\epsilon)^2. \quad (19)$$

It is hard to obtain analytical results for Eq. (15) and Eq. (18). Therefore, we need numerical evaluations. We can obtain the concurrence from Eq. (7) by evaluating the values of  $P_D$  and  $X$  (see Appendix A).

For the entanglement harvesting in the situation where two detectors are rotating with the same acceleration and trajectory radius, i.e.,  $a_A = a_B = a$ ,  $R_A = R_B = R$ . For simplicity, we consider that the two detectors are completely comoving ( $\omega_A = \omega_B = \omega$ ), therefore we obtain

$$X|_{a,R} = -\frac{\lambda^2\sigma^2 e^{-\sigma^2\Omega^2}}{2\pi^{3/2}\gamma} \int_0^\infty d\tilde{s} e^{-\tilde{s}^2/(4\gamma^2)} \left(\frac{1}{f(\tilde{s})|_{a,R}} - \frac{1}{f(\tilde{s})|_{a,R} + 4\Delta d\Delta z + 4\Delta z^2}\right), \quad (20)$$

where

$$f(\tilde{s})|_{a,R} = \Delta d^2 + 4R^2 \sin^2(\tilde{s}\omega\sigma/2) - \sigma^2(\tilde{s} + i\epsilon)^2. \quad (21)$$

For comparison with the case of linear uniformly accelerated motion, we consider the following trajectory for uniform acceleration

$$\begin{aligned} x_A &:= \{t = a^{-1} \sinh(a\tau_A), x = a^{-1} \cosh(a\tau_A), y = 0, z = \Delta z\}, \\ x_B &:= \{t = a^{-1} \sinh(a\tau_B), x = a^{-1} \cosh(a\tau_B), y = 0, z = \Delta z + \Delta d\}, \end{aligned} \quad (22)$$

where  $a$  still represents the magnitude of acceleration and  $\Delta d$  denotes the separation between two detectors.

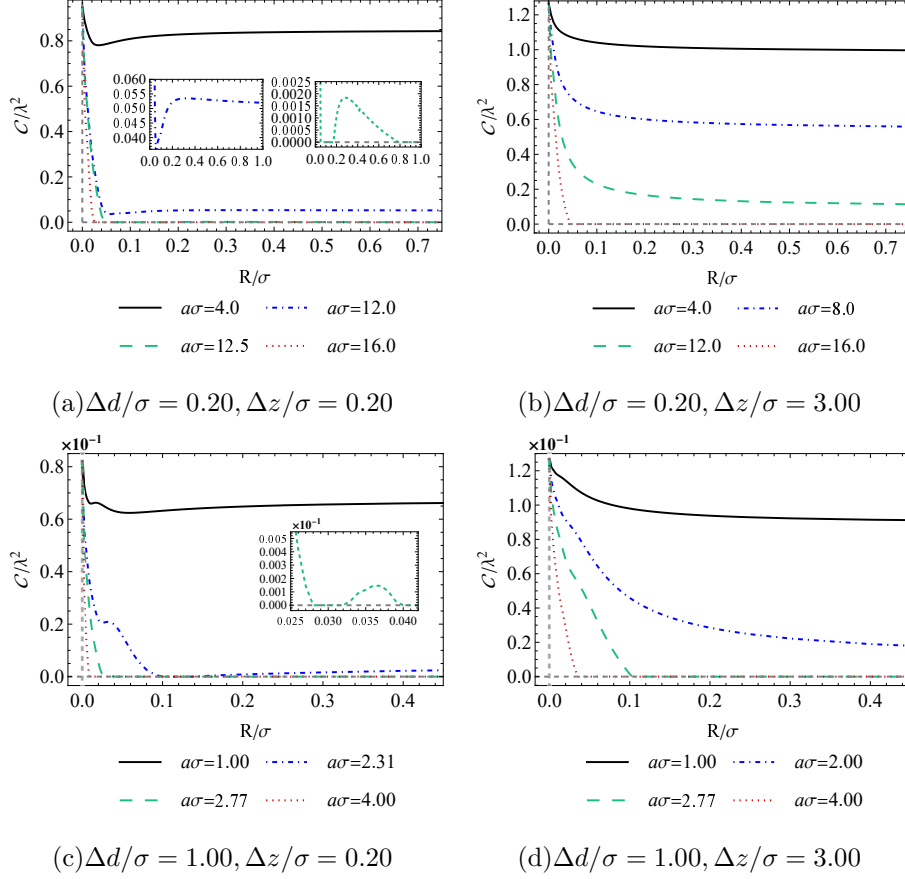


FIG. 5: The concurrence  $\mathcal{C}(\rho_{AB})/\lambda^2$  is plotted as a function of  $R/\sigma$  for different  $a\sigma$  with  $\Delta d/\sigma = \{0.20, 1.00\}$  and  $\Delta z/\sigma = \{0.20, 3.00\}$ . Here we have set  $\Omega\sigma = 0.10$ .

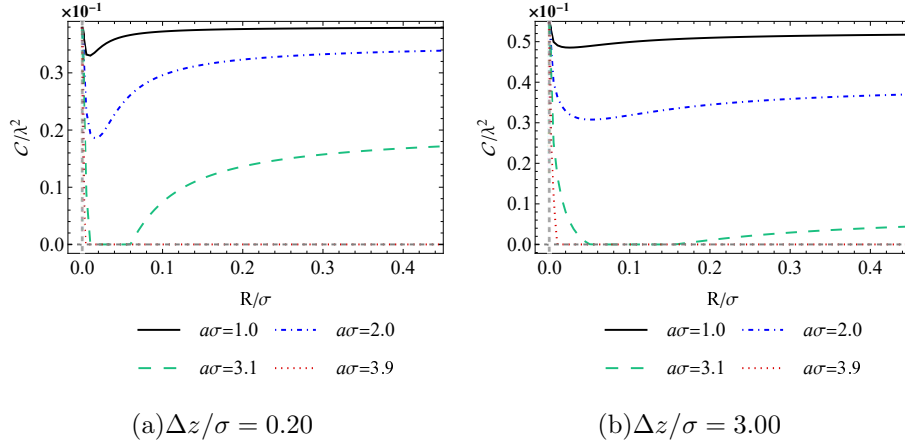


FIG. 6: The concurrence  $\mathcal{C}(\rho_{AB})/\lambda^2$  is plotted as a function of  $R/\sigma$  for different  $a\sigma$  with  $\Omega\sigma = 1.80$ ,  $\Delta d/\sigma = 0.20$  and  $\Delta z/\sigma = \{0.20, 3.00\}$ .

We depict the concurrence as a function of  $R/\sigma$  with a small  $\Omega\sigma = 0.10$  in Fig. 5 and a larger  $\Omega\sigma = 1.80$  in Fig. 6. For small  $\Delta d/\sigma = 0.20$  and small  $\Delta z/\sigma = 0.20$  in Fig. 5(a), the

entanglement (concurrence) in a very large  $a\sigma$  will quickly decrease to zero as  $R/\sigma$  increases. As we decrease  $a\sigma$ , the concurrence first decreases, then increases, but finally reduces to a stable value. Decreasing  $a\sigma$ , the concurrence first decreases, then increases to a stable value. For larger  $\Delta d/\sigma = 1.00$  and small  $\Delta z/\sigma = 0.20$  as shown in 5(c), with a not large  $a\sigma$ , the concurrence first decreases, then increases, then decreases, and finally increases to a stable value. The feature of large  $a\sigma$  is similar to the case of small  $\Delta d/\sigma$  and small  $\Delta z/\sigma$ . In Figs. 5(b) and 5(d), for a larger  $\Delta z/\sigma = 3.00$ , increasing  $R/\sigma$ , the concurrence decreases and finally arrives at a stable value. For a larger  $\Omega\sigma$  such as  $\Omega\sigma = 1.80$  in Fig. 6, there exist similar characteristics for any nonzero  $\Delta z/\sigma$ . For a very large  $a\sigma$ , the concurrence will decrease to zero. As we decrease  $a\sigma$ , the concurrence first decreases, then increases, and finally reaches a stable value. It should be noted that the concurrence in some situations first decreases to zero, then maintains zero, and finally increases to a stable value.

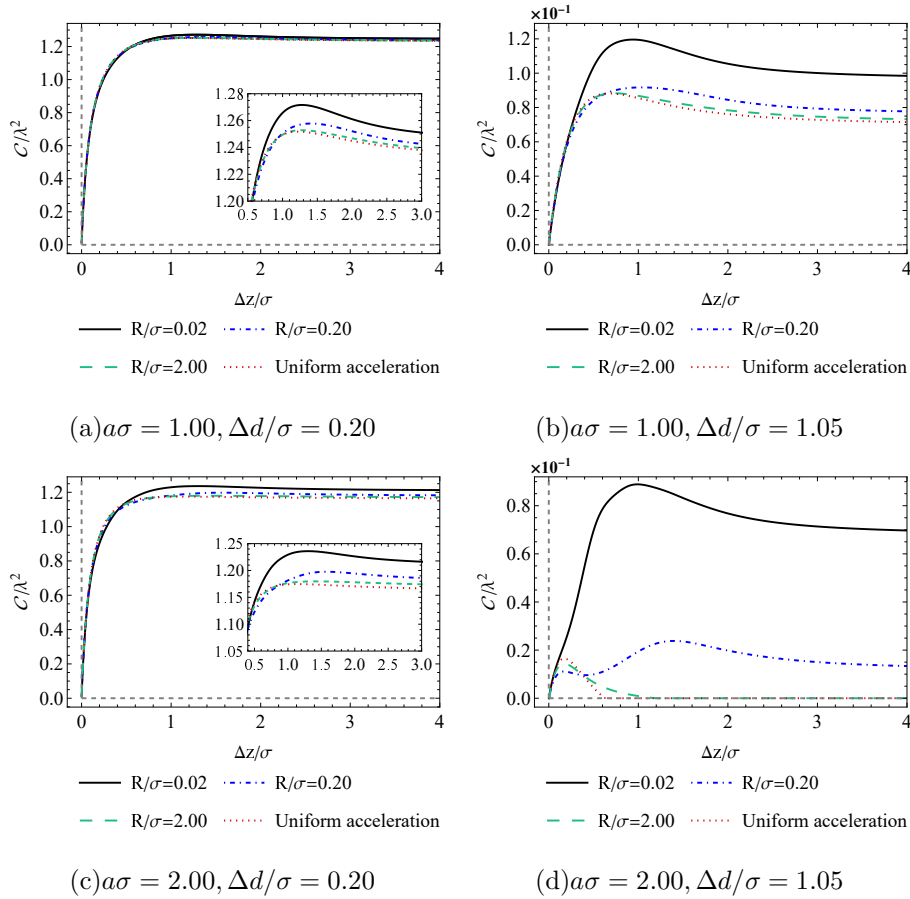


FIG. 7: The concurrence  $\mathcal{C}(\rho_{AB})/\lambda^2$  is plotted as a function of  $\Delta z/\sigma$  with different  $a\sigma$  and  $\Delta d/\sigma$ . We have set  $\Omega\sigma = 0.10$  for both circularly and uniformly accelerated motion.

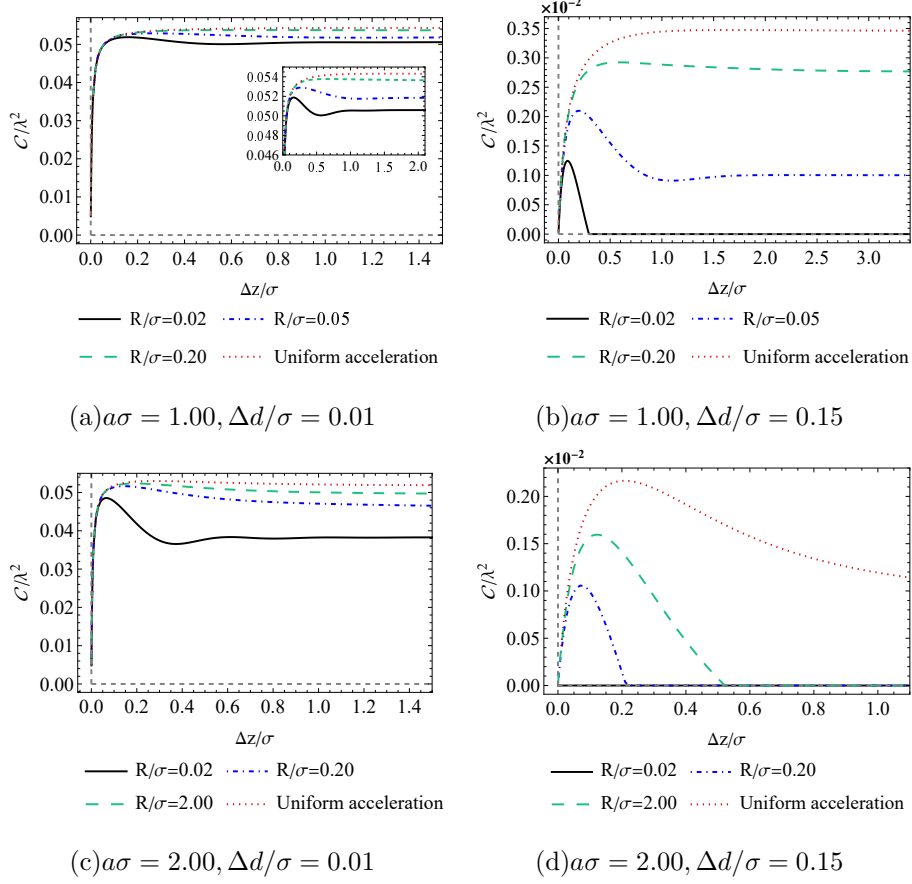


FIG. 8: The concurrence  $\mathcal{C}(\rho_{AB})/\lambda^2$  is plotted as a function of  $\Delta z/\sigma$  for different  $a\sigma$  and  $\Delta d/\sigma$ . We have set  $\Omega\sigma = 2.50$  for both circularly and uniformly accelerated motion.

In Fig. 7, we display the concurrence as a function of  $\Delta z/\sigma$  with a small  $\Omega\sigma = 0.10$ . For small  $\Delta d/\sigma = 0.20$  or small  $a\sigma = 1$ , the concurrence first increases, then decrease, and finally reaches a stable value. When we take a larger  $\Delta d/\sigma = 1.05$  and a not small  $a\sigma = 2.00$ , there may exist two peaks for some  $R/\sigma$ . In Fig. 8, we describe the concurrence as a function of  $\Delta z/\sigma$  for a larger  $\Omega\sigma = 2.50$ . There may exist more than one peak with a very small  $\Delta d/\sigma = 0.01$  or small  $a\sigma = 1$ . For not very small  $\Delta d/\sigma$  and not small  $a\sigma$ , there only exists no more than one peak.

We depict the concurrence as a function of  $\Omega\sigma$  for  $a\sigma = 1.00$  in Fig. 9. For a large  $\Omega\sigma$ , the concurrence goes to zero with any  $\Delta d/\sigma$  and  $\Delta z/\sigma$ . For  $\Delta d/\sigma = 0.50$ , the concurrence first increases from a nonzero value, then decreases to zero. As we amplify  $\Delta d/\sigma = 1.50$ , we observe that the concurrence with a small  $\Omega\sigma$  may take zero for a larger  $\Delta z/\sigma$  from Fig. 9(d). When we take a larger  $\Delta d/\sigma = 2.00$ , the concurrence with a small  $\Omega\sigma$  takes zero for

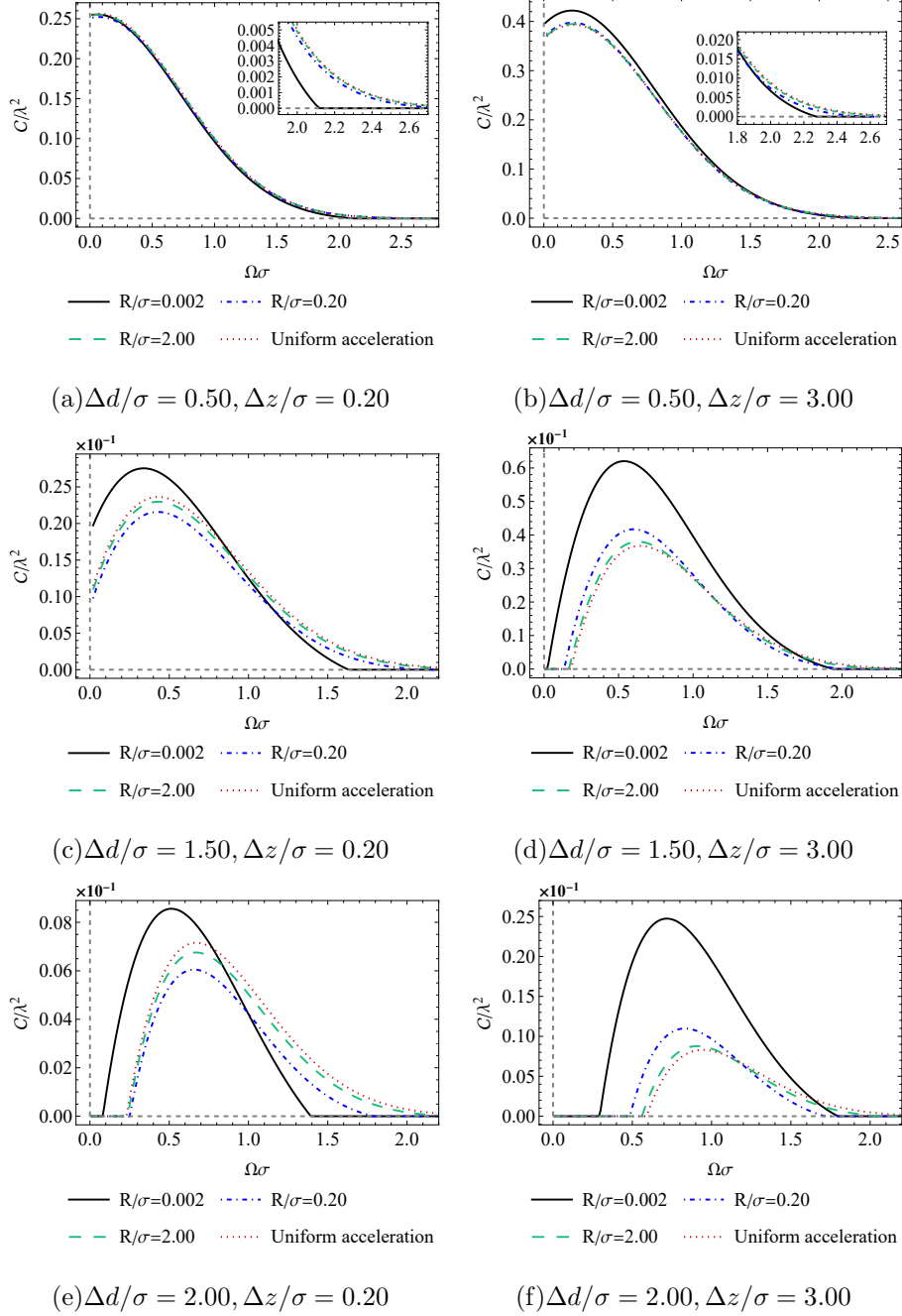


FIG. 9: The concurrence  $\mathcal{C}(\rho_{AB})/\lambda^2$  is plotted as a function of  $\Omega\sigma$  with  $\Delta d/\sigma = \{0.50, 1.50, 2.00\}$  and  $\Delta z/\sigma = \{0.20, 3.00\}$ . We have set  $a\sigma = 1.00$  for both circularly and uniformly accelerated motion.

any nonzero  $\Delta z/\sigma$ .

In Fig. 10, we describe the concurrence as a function of  $a\sigma$  with  $\Delta d/\sigma = 0.20$ . For a small  $\Delta z/\sigma = 0.20$ , the concurrence first increases, and then decreases to zero. There exists a peak value. For a larger  $\Delta z/\sigma = 3.00$ , as  $a\sigma$  increases, the concurrence decreases to zero.

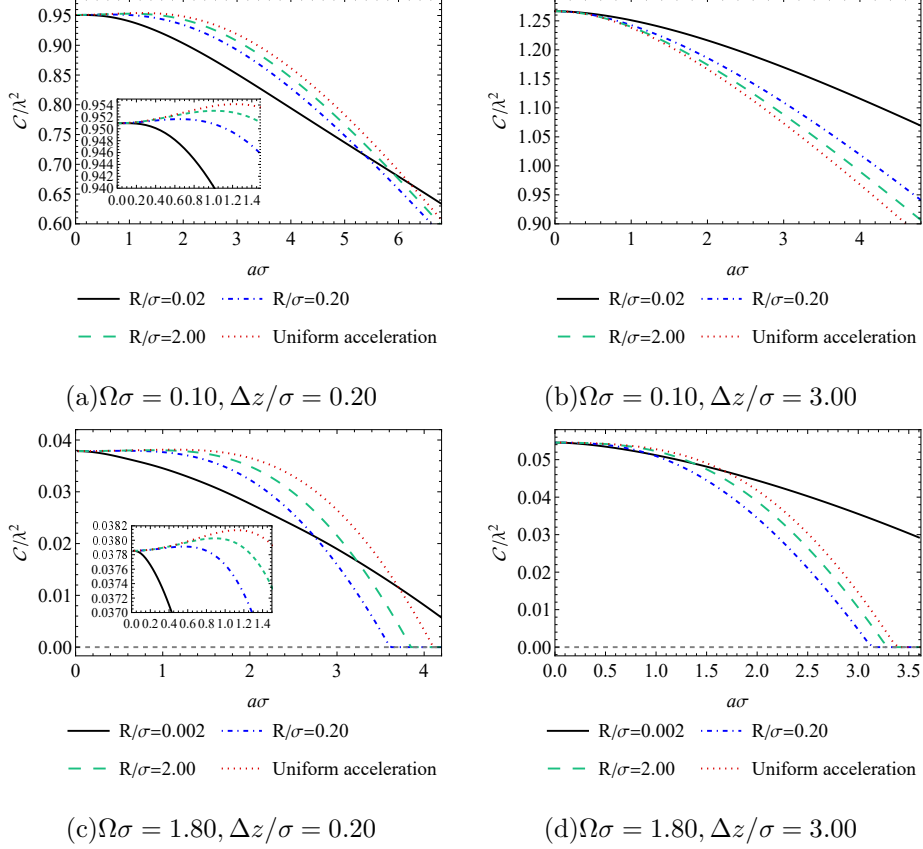


FIG. 10: The concurrence  $\mathcal{C}(\rho_{AB})/\lambda^2$  is plotted as a function of  $a\sigma$  with  $\Omega\sigma = \{0.10, 1.80\}$  and  $\Delta z/\sigma = \{0.20, 3.00\}$ . We have set  $\Delta d/\sigma = 0.20$  for both circularly and uniformly accelerated motion.

There is not intersection with nonzero  $a\sigma$  for small  $\Omega\sigma$  and larger  $\Delta z/\sigma$  as shown in Fig. 10(b). As  $\Delta d/\sigma$  increases, the concurrence goes to zero.

## V. CONCLUSION

In this paper, we have studied the properties of the transition probability of a circularly accelerated UDW detector coupled with massless scalar fields in a reflecting boundary. For a small  $\Omega\sigma$  and a small  $\Delta z/\sigma$ , with the increase of  $R_D/\sigma$ , the transition probability increases directly to a stable value for  $a_D\sigma > a_{D_c}\sigma$ . When we decrease  $a_D\sigma$ , the transition probability first increases, then decreases, and finally increases to a stable value. Decreasing  $a_D\sigma$ , the transition probability first increases, then decreases to a stable value. It will increase to a stable value with a larger  $\Delta z/\sigma$  for any nonzero  $a_D\sigma$ . For a larger  $\Omega\sigma$ , there will exist more

than one peak for some  $a_D\sigma$  and  $\Delta z/\sigma$ . Furthermore, for a small  $\Omega\sigma$ , there exists a critical value  $\Delta z_c/\sigma$ . When  $\Delta z/\sigma < \Delta z_c/\sigma$ , as we amplify  $a_D\sigma$ , a larger transition probability can be achieved first at a smaller trajectory radius, which is opposite to the case of large  $a_D\sigma$ . As  $\Delta z/\sigma$  increases, the intersections are shifted to the left. When  $\Delta z/\sigma > \Delta z_c/\sigma$ , a larger transition probability can be obtained for a larger trajectory radius with every nonzero  $a_D\sigma$ . However, with a larger  $\Omega\sigma > \Omega_c\sigma$ , the curves always exist intersections with different  $R_D/\sigma$  for any nonzero  $\Delta z/\sigma$ . The relation between the transition probability and  $\Omega\sigma$  has been considered. For a very large  $\Omega\sigma$ , the transition probability goes to zero. As  $\Delta z/\sigma$  increases, the intersections are shifted to the right until not move.

We also have investigated the entanglement harvesting phenomenon of two detectors with a boundary. We have discussed that the two detectors are rotating around a common axis with the same acceleration, trajectory radius and angular velocity. The relation between entanglement harvesting and  $R/\sigma$  has been taken into account. We first considered a small  $\Omega\sigma$ . For larger  $\Delta z/\sigma$ , the entanglement harvesting decreases and finally arrives at a stable value. For small  $\Delta d/\sigma$  and small  $\Delta z/\sigma$ , as  $R/\sigma$  increases, the entanglement harvesting in a very large  $a\sigma$  rapidly decays to zero. When  $a\sigma$  decreases, the entanglement harvesting first decreases, then increases, but finally decreases to a stable value. As we decrease  $a\sigma$ , the entanglement harvesting first decreases, then increases, and finally goes to a stable value. For large  $\Delta d/\sigma$  and small  $\Delta z/\sigma$ , with a not large  $a\sigma$ , the entanglement harvesting first decreases, then increases, then decreases, and finally increases to a stable value. The feature of large  $a\sigma$  is similar to that of small  $\Delta d/\sigma$  and small  $\Delta z/\sigma$ . We also considered a larger  $\Omega\sigma$ . For nonzero  $\Delta z/\sigma$ , the entanglement harvesting will decrease to zero with a large  $a\sigma$ . As we decrease  $a\sigma$ , the entanglement harvesting first decreases, then increases, and finally reaches a stable value. The influence of  $\Delta z/\sigma$  has been investigated. We first discussed a small  $\Omega\sigma$ . For small  $\Delta d/\sigma$  or small  $a\sigma$ , the entanglement harvesting first increases, then decrease, and finally arrives at a stable value. For not small  $a\sigma$  and larger  $\Delta d/\sigma$ , the entanglement harvesting may exist two peaks for some  $R/\sigma$ . For a larger  $\Omega\sigma$ , there may exist more than one peak with small  $a\sigma$  or very small  $\Delta d/\sigma$ . The entanglement harvesting is no more than one peak for not small  $a\sigma$  and not very small  $\Delta d/\sigma$ . The influence of  $\Omega\sigma$  for fixed  $a\sigma$  has been studied. For a large  $\Omega\sigma$ , the entanglement harvesting goes to zero. As  $\Delta d/\sigma$  increases, the entanglement harvesting with a larger  $\Delta z/\sigma$  may take zero at a small  $\Omega\sigma$ . For a larger  $\Delta d/\sigma$ , the entanglement harvesting with a small  $\Omega\sigma$  takes zero for any nonzero  $\Delta z/\sigma$ . We



have discussed the effect of  $a\sigma$  for not large  $\Delta d/\sigma$ . For a small  $\Delta z/\sigma$ , the entanglement harvesting first increases, and then decreases to zero. There exists a peak value. For a larger  $\Delta z/\sigma$ , as  $a\sigma$  increases, the entanglement harvesting decreases to zero. There is not intersection with a nonzero  $a\sigma$  for small  $\Omega\sigma$  and larger  $\Delta z/\sigma$ . As  $\Delta d/\sigma$  increases, the entanglement harvesting goes to zero.

## Acknowledgments

This work was supported by the Nature Science Foundation of Shaanxi Province, China under Grant No. 2023-JC-YB-016 and the National Natural Science Foundation of China under Grant No. 11705144.

## Appendix A: Derivation of $P_D$ and $X$

In this appendix, we derive  $P_D$  and  $X$  from Eq. (4) and Eq. (6) respectively.

### 1. The transition probability $P_D$

Setting  $u = \tau_D$  and  $s = \tau_D - \tau'_D$ , we have

$$\begin{aligned} P_D &= \lambda^2 \int_{-\infty}^{\infty} du \chi_D(u) \int_{-\infty}^{\infty} ds \chi_D(u-s) e^{-i\Omega s} W(s) \\ &= \lambda^2 \sqrt{\pi} \sigma \int_{-\infty}^{\infty} ds e^{-i\Omega s} e^{-s^2/(4\sigma^2)} W(s). \end{aligned} \quad (\text{A1})$$

Inserting Eq. (10) into Eq. (A1) and using  $x = \gamma_D |\omega_D| s/2$ , the transition probability can be written as  $P_D = P_1 + P_2$ . The first term read

$$P_1 = \frac{\lambda^2 \sigma |\omega_D|}{8\pi^{3/2} \gamma_D} \int_{-\infty}^{\infty} dx \frac{e^{-ix\beta} e^{-x^2\alpha}}{v_D^2 \sin^2 x - (x - i\epsilon)^2}, \quad (\text{A2})$$

and the second term can be written as

$$P_2 = \frac{\lambda^2 \sigma |\omega_D|}{8\pi^{3/2} \gamma_D} \int_{-\infty}^{\infty} dx \frac{e^{-ix\beta} e^{-x^2\alpha}}{(x - i\epsilon)^2 - v_D^2 \sin^2 x - \omega_D^2 \Delta z^2}, \quad (\text{A3})$$

where  $\alpha := 1/(\sigma^2 \omega_D^2 \gamma_D^2)$ ,  $\beta := 2\Omega/(\gamma_D |\omega_D|)$ .  $P_1$  can be rewritten as

$$\begin{aligned} P_1 &= \frac{\lambda^2 \sigma |\omega_D|}{8\pi^{3/2} \gamma_D} \int_{-\infty}^{\infty} dx \left[ \frac{e^{-ix\beta} e^{-x^2\alpha}}{v_D^2 \sin^2 x - (x - i\epsilon)^2} + \frac{e^{-ix\beta} e^{-x^2\alpha}}{(1 - v_D^2)(x - i\epsilon)^2} - \frac{e^{-ix\beta} e^{-x^2\alpha}}{(1 - v_D^2)(x - i\epsilon)^2} \right] \\ &= K_D \int_0^{\infty} dx \frac{\cos(x\beta) e^{-x^2\alpha} (x^2 - \sin^2 x)}{x^2 (x^2 - v_D^2 \sin^2 x)} - \frac{\lambda^2 \sigma |\omega_D|}{8\pi^{3/2} \gamma_D} \int_{-\infty}^{\infty} dx \frac{e^{-ix\beta} e^{-x^2\alpha}}{(1 - v_D^2)(x - i\epsilon)^2}, \end{aligned} \quad (\text{A4})$$

where  $K_D := \lambda^2 v_D^2 \gamma_D |\omega_D| \sigma / (4\pi^{3/2})$ . In second line of Eq. (A4), we have neglected  $i\epsilon$  since the integral is now regular. The second term can be expressed as

$$\begin{aligned} & - \frac{\lambda^2 \sigma |\omega_D|}{8\pi^{3/2} \gamma_D} \int_{-\infty}^{\infty} dx \frac{e^{-ix\beta} e^{-x^2\alpha}}{(1-v_D^2)(x-i\epsilon)^2} \\ & = - \frac{\lambda^2 \sigma \gamma_D |\omega_D|}{8\pi^{3/2}} \int_{-\infty}^{\infty} dx \frac{e^{-ix\beta} e^{-x^2\alpha}}{x^2} + \frac{i\lambda^2 \sigma \gamma_D |\omega_D|}{8\pi^{1/2}} \int_{-\infty}^{\infty} dx e^{-ix\beta} e^{-x^2\alpha} \delta^{(1)}(x). \end{aligned} \quad (\text{A5})$$

We have used the following identity,

$$\frac{1}{(x \pm i\epsilon)^n} = \frac{1}{x^n} \pm \frac{(-1)^n}{(n-1)!} i\pi \delta^{(n-1)}(x). \quad (\text{A6})$$

Considering the definition of a distribution  $g$  acting on a test function  $f$

$$\langle g, f \rangle := \int_{-\infty}^{\infty} g(x) f(x) dx, \quad (\text{A7})$$

we have the following identities for a distribution function [27, 41]

$$\left\langle \frac{1}{x}, f(x) \right\rangle = \text{PV} \int_{-\infty}^{\infty} \frac{f(x)}{x} dx, \quad (\text{A8})$$

$$\left\langle \frac{1}{x^2}, f(x) \right\rangle = \int_0^{\infty} dx \frac{f(x) + f(-x) - 2f(0)}{x^2}, \quad (\text{A9})$$

and

$$\langle \delta^{(n)}(x), f(x) \rangle = (-1)^n f^{(n)}(0), \quad (\text{A10})$$

where PV is the principle value of an integral. Therefore, by using Eq. (A9) and Eq. (A10), Eq. (A5) can be rewritten as

$$- \frac{\lambda^2 \sigma |\omega_D|}{8\pi^{3/2} \gamma_D} \int_{-\infty}^{\infty} dx \frac{e^{-ix\beta} e^{-x^2\alpha}}{(1-v_D^2)(x-i\epsilon)^2} = \frac{\lambda^2}{4\pi} \left[ e^{-\Omega^2 \sigma^2} - \sqrt{\pi} \Omega \sigma \text{Erfc}(\Omega \sigma) \right]. \quad (\text{A11})$$

$P_2$  can be expressed as

$$\begin{aligned} P_2 & = \frac{\lambda^2 \sigma |\omega_D|}{8\pi^{3/2} \gamma_D} \left[ \int_{-\infty}^0 dx \frac{e^{-ix\beta} e^{-x^2\alpha}}{x^2 - v_D^2 \sin^2 x - \omega_D^2 \Delta z^2 + i\epsilon} + \int_0^{\infty} dx \frac{e^{-ix\beta} e^{-x^2\alpha}}{x^2 - v_D^2 \sin^2 x - \omega_D^2 \Delta z^2 - i\epsilon} \right] \\ & = \frac{\lambda^2 \sigma |\omega_D|}{4\pi^{3/2} \gamma_D} \text{PV} \int_0^{\infty} dx \frac{\cos(x\beta) e^{-x^2\alpha}}{x^2 - v_D^2 \sin^2 x - \omega_D^2 \Delta z^2} + \frac{\lambda^2 \sigma |\omega_D|}{4\sqrt{\pi} \gamma_D} \frac{e^{-S^2\alpha} \sin(S\beta)}{2S - v_D^2 \sin 2S}, \end{aligned} \quad (\text{A12})$$

where  $S$  is the solution of  $x^2 - v_D^2 \sin^2 x - \omega_D^2 \Delta z^2 = 0$ . We can obtain the expression of the transition probability given in Eq. (11).

## 2. The expression of $X$

From the definition of  $X$  in Eq. (6), we have

$$\begin{aligned}
X &= -\frac{\lambda^2}{\gamma_A \gamma_B} \int_{-\infty}^{\infty} dt \int_{-\infty}^t dt' \left[ \chi_B(\tau_B(t)) \chi_A(\tau_A(t')) e^{-i(\Omega t / \gamma_B + \Omega t' / \gamma_A)} W(x_A(t'), x_B(t)) \right. \\
&\quad \left. + \chi_A(\tau_A(t)) \chi_B(\tau_B(t')) e^{-i(\Omega t / \gamma_A + \Omega t' / \gamma_B)} W(x_B(t'), x_A(t)) \right] \\
&= -\frac{\lambda^2 \sigma^2}{\gamma_A \gamma_B} \int_{-\infty}^{\infty} d\tilde{u} \int_0^{\infty} d\tilde{s} \left[ e^{-\tilde{u}^2(\gamma_B^{-2} + \gamma_A^{-2})/2} e^{-\tilde{s}^2/2\gamma_A^2} e^{\tilde{s}\tilde{u}/\gamma_A^2} e^{-i\tilde{u}\Omega\sigma[\gamma_B^{-1} + \gamma_A^{-1}]} e^{i\tilde{s}\Omega\sigma/\gamma_A} W(x_A(t'), x_B(t)) \right. \\
&\quad \left. + e^{-\tilde{u}^2(\gamma_A^{-2} + \gamma_B^{-2})/2} e^{-\tilde{s}^2/2\gamma_B^2} e^{\tilde{s}\tilde{u}/\gamma_B^2} e^{-i\tilde{u}\Omega\sigma[\gamma_A^{-1} + \gamma_B^{-1}]} e^{i\tilde{s}\Omega\sigma/\gamma_B} W(x_B(t'), x_A(t)) \right], \quad (\text{A13})
\end{aligned}$$

where we have used  $\tilde{u} = t/\sigma$ ,  $\tilde{s} = (t - t')/\sigma$ . In particular, if the Wightman function is only dependent on  $\tilde{s}$ , Eq. (A13) can be further expressed as

$$\begin{aligned}
X &= -\frac{\sqrt{2\pi}\lambda^2\sigma^2}{\sqrt{\gamma_A^2 + \gamma_B^2}} \exp\left[\frac{-\sigma^2\Omega^2(\gamma_A + \gamma_B)^2}{2\gamma_A^2 + 2\gamma_B^2}\right] \int_0^{\infty} d\tilde{s} \left\{ \exp\left[\frac{i\tilde{s}\sigma\Omega(\gamma_A - \gamma_B)}{\gamma_A^2 + \gamma_B^2}\right] \exp\left[\frac{-\tilde{s}^2}{2(\gamma_A^2 + \gamma_B^2)}\right] \right. \\
&\quad \left. \times W(x_A(t'), x_B(t)) + \exp\left[\frac{i\tilde{s}\sigma\Omega(\gamma_B - \gamma_A)}{\gamma_A^2 + \gamma_B^2}\right] \exp\left[\frac{-\tilde{s}^2}{2(\gamma_A^2 + \gamma_B^2)}\right] W(x_B(t'), x_A(t)) \right\}. \quad (\text{A14})
\end{aligned}$$

Using the explicit expression of the Wightman function, one can obtain Eq. (18) and Eq. (20).

- 
- [1] J. von Neumann, *Mathematische Grundlagen der Quantenmechanik* (Springer Berlin, Heidelberg, Germany, 1932).
  - [2] A. Einstein, B. Podolsky and N. Rosen, Can quantum-mechanical description of physical reality be considered complete? *Phys. Rev.* **47**, 777 (1935).
  - [3] E. Schrödinger, Die gegenwärtige situation in der quantenmechanik, *Naturwissenschaften* **23**, 807812 (1935).
  - [4] E. Schrödinger, Discussion of probability relations between separated systems, *Mathematical Proceedings of the Cambridge Philosophical Society* **31** (4): 555563 (1935).
  - [5] C. S. Wu and I. Shakhov, The angular correlation of scattered annihilation radiation, *Phys. Rev.* **77**, 136 (1950).
  - [6] D. Bohm, *Quantum Theory* (Prentice Hall, Englewood Cliffs, New Jersey, 1951).

- [7] D. Bohm, A Suggested interpretation of the quantum theory in terms of “hidden” variables. I; A suggested interpretation of the quantum theory in terms of “hidden” variables. II, *Phys. Rev.* **85**, 166; 180 (1952).
- [8] D. Bohm and Y. Aharonov, Discussion of experimental proof for the paradox of Einstein, Rosen, and Podolsky, *Phys. Rev.* **108**, 1070 (1957).
- [9] J. S. Bell, On the Einstein Podolsky Rosen paradox, *Physics Physique Fizika* **1**, 195 (1964).
- [10] S. J. Freedman and J. F. Clauser, Experimental test of local hidden-variable theories, *Phys. Rev. Lett.* **28**, 938 (1972).
- [11] A. Aspect, P. Grangier, and G. Roger, Experimental realization of Einstein-Podolsky-Rosen-Bohm gedankenexperiment: A new violation of Bell’s inequalities, *Phys. Rev. Lett.* **49**, 91 (1982).
- [12] A. Aspect, J. Dalibard, and G. Roger, Experimental test of Bell’s inequalities using time-varying analyzers, *Phys. Rev. Lett.* **49**, 1804 (1982).
- [13] D. Bouwmeester, J. W. Pan, K. Mattle, M. Eibl, H. Weinfurter, and A. Zeilinger, Experimental quantum teleportation, *Nature* **390**, 575 (1997).
- [14] S. J. Summers and R. Werner, The vacuum violates Bell’s inequalities, *Phys. Lett. A* **110**, 257 (1985).
- [15] S. J. Summers and R. Werner, Bell’s inequalities and quantum field theory. I. General setting, *J. Math. Phys.* **28**, 2440 (1987).
- [16] S. J. Summers and R. Werner, Bell’s inequalities and quantum field theory. II. Bell’s inequalities are maximally violated in the vacuum, *J. Math. Phys.* **28**, 2448 (1987).
- [17] A. Valentini, Non-local correlations in quantum electrodynamics, *Phys. Lett. A* **153**, 321 (1991).
- [18] B. Reznik, Entanglement from the vacuum, *Found. Phys.* **33**, 167 (2003).
- [19] B. Reznik, A. Retzker and J. Silman, Violating Bell’s inequalities in vacuum, *Phys. Rev. A* **71**, 042104 (2005).
- [20] G. V. Steeg and N. C. Menicucci, Entangling power of an expanding universe, *Phys. Rev. D* **79**, 044027 (2009).
- [21] S. J. Olson and T. C. Ralph, Entanglement between the future and the past in the quantum vacuum, *Phys. Rev. Lett.* **106**, 110404 (2011).
- [22] E. Martín-Martínez and N. C. Menicucci, Cosmological quantum entanglement, *Class. Quant.*

- Grav. **29**, 224003 (2012).
- [23] B. L. Hu, S.-Y. Lin and J. Louko, Relativistic quantum information in detectors-field interactions, *Class. Quant. Grav.* **29**, 224005 (2012).
- [24] E. Martín-Martínez, E. G. Brown, W. Donnelly and A. Kempf, Sustainable entanglement production from a quantum field, *Phys. Rev. A* **88**, 052310 (2013).
- [25] G. Salton, R. B. Mann and N. C. Menicucci, Acceleration-assisted entanglement harvesting and ranging, *New J. Phys.* **17**, 035001 (2015).
- [26] A. Pozas-Kerstjens and E. Martín-Martínez, Harvesting correlations from the quantum vacuum, *Phys. Rev. D* **92**, 064042 (2015).
- [27] E. Martín-Martínez, A. R. H. Smith and D. R. Terno, Spacetime structure and vacuum entanglement, *Phys. Rev. D* **93**, 044001 (2015).
- [28] E. Martín-Martínez and B. C. Sanders, Precise space-time positioning for entanglement harvesting, *New J. Phys.* **18**, 043031 (2016).
- [29] L. J. Henderson, R. A. Hennigar, R. B. Mann, A. R. H. Smith and J. Zhang, Harvesting entanglement from the black hole vacuum, *Class. Quant. Grav.* **35**, 21LT02 (2018).
- [30] L. J. Henderson, R. A. Hennigar, R. B. Mann, A. R. H. Smith and J. Zhang, Entangling detectors in anti-de Sitter space, *J. High Energ. Phys.* **05**, 178 (2019).
- [31] W. Cong, E. Tjoa and R. B. Mann, Entanglement harvesting with moving mirrors, *J. High Energ. Phys.* **06**, 021 (2019).
- [32] Jun-ichirou Koga, K. Maeda and G. Kimura, Entanglement extracted from vacuum into accelerated Unruh-DeWitt detectors and energy conservation, *Phys. Rev. D* **100**, 065013 (2019).
- [33] J. Zhang and H. Yu, Entanglement harvesting for Unruh-DeWitt detectors in circular motion, *Phys. Rev. D* **102**, 065013 (2020).
- [34] W. Cong, C. Qian, M. R. R. Good and R. B. Mann, Effects of horizons on entanglement harvesting, *J. High Energ. Phys.* **10**, 067 (2020).
- [35] Z. Liu, J. Zhang and H. Yu, Entanglement harvesting in the presence of a reflecting boundary, *J. High Energ. Phys.* **08**, 020 (2021).
- [36] B. S. DeWitt, S. Hawking and W. Israel, *General Relativity: An Einstein Centenary Survey* (Cambridge University Press, Cambridge, England, 1979).
- [37] W. K. Wootters, Entanglement of formation of an arbitrary state of two qubits, *Phys. Rev. Lett.* **80**, 2245 (1998).

- [38] N. D. Birrell and P. C. W. Davies, *Quantum Fields in Curved Space*, Cambridge Monographs on Mathematical Physics (Cambridge University Press, Cambridge, England, 1984).
- [39] L. C. B. Crispino, A. Higuchi, G. E. A. Matsas, The Unruh effect and its applications, *Rev. Mod. Phys.* **80**, 787 (2008).
- [40] L. Rizzuto and S. Spagnolo, Energy level shifts of a uniformly accelerated atom in the presence of boundary conditions, *J. Phys. Conf. Ser.* **161**, 012031 (2009).
- [41] N. N. Bogolubov, A. A. Logunov, A. I. Oksak, and I. T. Todorov, *General Principles of Quantum Field Theory* (Springer, New York, 1990).